R. & M. No. 3467

MINISTRY OF TECHNOLOGY

AERONAUTICAL RESEARCH COUNCIL
REPORTS AND MEMORANDA

A Numerical Method for Solving the Equations for a Vortex Core

by M. G. HALL

LONDON: HER MAJESTY'S STATIONERY OFFICE
1967
PRICE 14*s.* 0*d.* NET

A Numerical Method for Solving the Equations for a Vortex Core

by M. G. HALL

Reports and Memoranda No. 3467*
May, 1965

Summary.

A method is presented for calculating steady axially symmetric spiralling motions of an incompressible fluid at large Reynolds numbers. By making approximations of the boundary-layer type the Navier-Stokes equations are reduced essentially to a pair of non-linear parabolic equations. Initial conditions are specified on some upstream cross-section, and boundary conditions on the axis of symmetry and on some bounding surface of revolution. The method involves replacing the differential equations by sets of finite-difference equations, using first-order central differences in an implicit scheme. The calculation is by a marching technique, which proceeds step-by-step in the axial direction. For each step an iterative plan is followed. The finite-difference equations themselves are solved by straightforward matrix methods. A programme is developed for a digital computer of moderate size and examples of the application of the method are given.

LIST OF CONTENTS

Section

1. Introduction
2. The Basic Differential Equations
3. New Variables. Initial and Boundary Conditions
4. The Difference Equations and the Method of Solution
   - 4.1. The difference approximations
   - 4.2. The basic difference equations
   - 4.3. The basic cycle of computations
   - 4.4. An outer iteration
   - 4.5. A proceedure for cases of specified boundary shape
5. Examples
   - 5.1. General features of the computations
   - 5.2. A trailing vortex
   - 5.3. A leading-edge vortex
   - 5.4. A vortex in a pipe

*Replaces R.A.E. Tech. Report No. 65 106—A.R.C. 27 150.

LIST OF CONTENTS—*continued*

6. Discussion

Table 1 Effect of mesh size on computed values for a leading-edge vortex

Table 2 Effect of mesh size on computed values for a vortex in a pipe

Symbols

References

Illustrations—Figs. 1–10

Detachable Abstract Cards

---

1. *Introduction.*

Vortices are found in a variety of conditions; they can be observed for example in wakes, over the leading edges of highly-swept wings, and in pipes, and also in nature as hurricanes, tornadoes and whirlpools. However, no general method for calculating their structure exists, partly because the conditions in which they occur are themselves not well understood and partly because the governing differential equations are both non-linear and elliptic. On the other hand, many vortices possess a roughly axially-symmetric core of spiralling fluid and the structure of such cores is frequently more amenable to treatment. If variations in the axial direction are small compared with those in the radial direction the equations can be reduced to parabolic equations of the boundary-layer type. Such flows, called quasi-cylindrical, are considered here.

If the flow is inviscid as well as quasi-cylindrical the problem can be reduced (*see* for example Ref. 1) to that of solving an ordinary differential equation for the stream function. The solution is still far from trivial, because the equation is generally non-linear and the boundary conditions are of the two-point type. In any case it can have only a limited applicability to real flows, like other inviscid solutions. In fact there are phenomena in which viscous diffusion plays a decisive role, such as the decay of a trailing vortex, and phenomena where the role of viscosity is uncertain, such as vortex breakdown. A method of calculation is presented here for the steady spiralling motion of a viscous incompressible fluid, where the velocity field is axially symmetric and approximations of the boundary-layer type can be made. Although the physical significance of the basic differential equations and their boundary conditions receives some attention, the main concern here is with numerical technique and not physical interpretation. The latter is discussed by Hall in a review[1] of recent work on the structure of concentrated vortex cores. In addition to direct numerical solution the method may be used for numerical "experiments" with vortex cores, by observing the effects of varying initial and boundary conditions. This may be useful for studying the physical properties of the vortex cores.

The differential equations for which a general method of solution is given here have been considered before. In an attempt to treat trailing vortices with appreciable swirl Gartshore[2] has substituted polynomials for the profiles of the axial and circumferential components of velocity, and obtained approximate solutions of an integral form of the equations in the Pohlhausen manner. Stewartson and Hall[3] have obtained a solution for the core of a leading-edge vortex in the form of an asymptotic expansion containing inverse powers of the logarithm of a Reynolds number. These solutions are highly specialised and Gartshores' in addition suffers from the usual limitations of integral methods. They are included in Hall's review[1]. A related set of equations has been considered by Abbott[4] who developed a numerical method of solution with such success as to encourage the present author to begin the work described here.

The implicit finite-difference technique used here is similar to that developed by Hartree[5], Leigh[6] and others[7,8] for calculating two-dimensional laminar boundary layers*. There, the problem reduces essentially to the numerical solution of a single non-linear parabolic equation. The solution is obtained by the step-by-step technique of marching along the surface: for each step the differential equation is replaced by a set of difference equations, one equation for each transverse pivotal point. The method is an implicit one, using first-order central differences defined so that the difference equations must be solved simultaneously. Such a procedure is stable for all step sizes when applied to the simple linear heat-diffusion equation, but for non-linear parabolic equations it has not yet been possible to prove stability, so solutions have to be checked individually. However, it has been found by experience that stability limitations are negligible. The non-linear difference equations are solved by iteration. Again, there is no proof that the iteration will converge.

In the present problem there are two non-linear parabolic equations instead of one, and they require simultaneous solution. It is possible in the interative process here, however, to avoid having to solve the two corresponding sets of difference equations simultaneously; in each cycle two sets of linear difference equations are solved successively. The cycle is repeated until results from successive cycles agree, that is, differ by less than some prescribed small amount. This convergence of the iteration is one of the main conclusions of the present work. Also, the boundary conditions in the present problem differ from those applying to boundary layers, and this has led to further differences in the method of solution.

The account which follows begins with a derivation of the basic differential equations. New variables are chosen, for convenience in computation, and initial and boundary conditions are discussed. Then the difference equations are set up and their solution is described. Finally, to illustrate its use in a variety of conditions, the method is applied to a trailing vortex, to a leading-edge vortex and to a vortex in a pipe. Checks are made by varying the mesh size in the difference approximations.

2. *The Basic Differential Equations.*

When the velocity field is axially symmetric, the non-dimensional form of the equations for the steady motion of an incompressible fluid is, without approximation,

$$u\frac{\partial(rv)}{\partial x}+w\frac{\partial(rv)}{\partial r}=\frac{\nu}{ql}\left[\nabla^2(rv)-\frac{2}{r}\frac{\partial(rv)}{\partial r}\right] \tag{1a}$$

$$u\frac{\partial u}{\partial x}+w\frac{\partial u}{\partial r}=-\frac{\partial P}{\partial x}+\frac{\nu}{ql}\nabla^2 u \tag{1b}$$

$$u\frac{\partial w}{\partial x}+w\frac{\partial w}{\partial r}-\frac{v^2}{r}=-\frac{\partial P}{\partial r}-\frac{\nu}{ql}\left(\nabla^2 w-\frac{w}{r^2}\right) \tag{1c}$$

$$\frac{\partial u}{\partial x}+\frac{\partial w}{\partial r}+\frac{w}{r}=0\,; \tag{1d}$$

where

$$\nabla^2\equiv\frac{\partial^2}{\partial r^2}+\frac{1}{r}\frac{\partial}{\partial r}+\frac{\partial^2}{\partial x^2}\,;$$

---

* Explicit techniques have also been used for boundary-layer calculations. They are much simpler in principle but are subject to numerical instability and are not considered here.

the cylindrical co-ordinates r,x are ratios of actual length to the reference length l; u,v and w are the ratios of the axial, circumferential and radial components of velocity, respectively, to the reference velocity q; P is the ratio of the pressure to ($q^2 \times$ density); and ν is the kinematic viscosity.

As in boundary-layer theory we now introduce the Reynolds number $Re = ql/\nu$ and the stretched variables $R = Re^{\frac{1}{2}}r$, $W = Re^{\frac{1}{2}}w$. The equations (1) become

$$\left.\begin{aligned} u\frac{\partial(Rv)}{\partial x}+W\frac{\partial(Rv)}{\partial R} &= \frac{\partial^2(Rv)}{\partial R^2}-\frac{1}{R}\frac{\partial(Rv)}{\partial R}+\frac{1}{Re}\frac{\partial^2(Rv)}{\partial x^2} \\ u\frac{\partial u}{\partial x}+W\frac{\partial u}{\partial R} &= -\frac{\partial P}{\partial x}+\frac{\partial^2 u}{\partial R^2}+\frac{1}{R}\frac{\partial u}{\partial R}+\frac{1}{Re}\frac{\partial^2 u}{\partial x^2} \\ \frac{u}{Re}\frac{\partial W}{\partial x}+\frac{W}{Re}\frac{\partial W}{\partial R}-\frac{v^2}{R} &= -\frac{\partial P}{\partial R}+\frac{1}{Re}\left(\frac{\partial^2 W}{\partial R^2}+\frac{1}{R}\frac{\partial W}{\partial R}-\frac{W}{R^2}+\frac{1}{Re}\frac{\partial^2 W}{\partial x^2}\right) \\ \frac{\partial u}{\partial x}+\frac{\partial W}{\partial R}+\frac{W}{R} &= 0. \end{aligned}\right\} \tag{2}$$

On making the usual boundary-layer approximation that at large Reynolds numbers all terms containing the factor $1/Re$ may be omitted we obtain the equations

$$u\frac{\partial(Rv)}{\partial x}+W\frac{\partial(Rv)}{\partial R} = \frac{\partial^2(Rv)}{\partial R^2}-\frac{1}{R}\frac{\partial(Rv)}{\partial R} \tag{3a}$$

$$u\frac{\partial u}{\partial x}+W\frac{\partial u}{\partial R} = -\frac{\partial P}{\partial x}+\frac{\partial^2 u}{\partial R^2}+\frac{1}{R}\frac{\partial u}{\partial R} \tag{3b}$$

$$\frac{v^2}{R} = \frac{\partial P}{\partial R} \tag{3c}$$

$$\frac{\partial u}{\partial x}+\frac{\partial W}{\partial R}+\frac{W}{R} = 0. \tag{3d}$$

These are the basic equations for which a method of solution is sought. The approximation, and the flow to which it applies, is called quasi-cylindrical.

There are two assumptions made in deriving the above. The first is that the Reynolds number Re is large. Corresponding solutions of the exact and approximate equations, (1) and (3), will be identical only in the limit $Re\to\infty$, or in the limit $\nu\to 0$. It is expected, however, from experience with boundary layers, that for sufficiently large finite Reynolds numbers a solution of (3) will closely approximate the corresponding solution of (1). The second assumption is that for each equation of the set (2) all the terms are the same order of magnitude, except those containing the factor $1/Re$, and they are assumed to be smaller in order of magnitude by this factor. Since the radial co-ordinates have been stretched relative to the axial ones this is equivalent to the assumption that variations in the axial direction are small compared with variations in the radial direction. It may be observed that one of the implications of this assumption is that the radial component of velocity and its derivatives must in general be small. Whether the second assumption is justified in any given case can be decided at present only by examination of the actual solution. We may conjecture, from the experience with boundary layers, that the solutions obtained will be compatible with the assumption made except near stagnation or reversal of the axial flow.

The qualities P and W can be eliminated from equations (3a) and (3b) by treating (3c) and (3d) as equations for P and W respectively. Equations (3a) and (3b) would then be a pair of equations to be

solved simultaneously for u and v. Note that although an approximation of the boundary-layer type has been made the equations are not linked together in the same way as the equations of a three-dimensional boundary layer. In ordinary boundary-layer theory the pair of equations for the two velocity components tangential to the surface are linked only through the inertia terms: the pressure terms are completely independent, being specified by the external flow. For the spiralling flow here the pressure term in equation (3b) depends on the magnitude of the circumferential velocity v: there is an additional link between the equation for u (3b) and that for v (3a), so that the interaction between the two velocity components will be more marked, and it is plausible that rapid changes can occur in the structure of a vortex as we proceed downstream. The equations are nevertheless parabolic and this suggests a numerical solution by marching, step-by-step, in the downstream direction.

3. *New Variables. Initial and Boundary Conditions.*

Let the surface of revolution bounding the vortex core, on which boundary conditions are given, be denoted by $r = r_b(x)$, and let $x = x_i$ denote the upstream cross-section on which the initial conditions are given. The surface $r = r_b(x)$ is not necessarily specified in advance of computation, and it need not be a solid surface or a stream surface. It is convenient to introduce the ratio $\lambda = r_b(x)/r_b(x_i)$ which describes the shape of the bounding surface, and to substitute for R, v and W new variables ζ, k and h defined by

$$\left.\begin{aligned} \zeta \equiv R/\lambda &= Re^{\frac{1}{2}} r/\lambda \\ k \equiv \lambda\zeta v &= Re^{\frac{1}{2}} rv \\ h \equiv W/\lambda &= Re^{\frac{1}{2}} w/\lambda\,. \end{aligned}\right\} \tag{4}$$

Thus at $r = r_b(x)$, $\zeta = \zeta_b = Re^{\frac{1}{2}} r_b(x_i) =$ constant so that the domain of computation $0 \geqslant r \geqslant r_b(x)$, $x \geqslant x_i$, is reduced to the simple open-ended rectangle $0 \geqslant \zeta \geqslant \zeta_b$, $x \geqslant x_i$. The quantity k is proportional to the circulation: k is constant on a stream tube if there is no diffusion across it.

On making the substitutions, equations (3) are transformed to

$$u\frac{\partial k}{\partial x} - \frac{1}{\lambda^2}\frac{\partial^2 k}{\partial \zeta^2} + \left(h - \frac{\lambda'}{\lambda}\zeta u + \frac{1}{\lambda^2\zeta}\right)\frac{\partial k}{\partial \zeta} = 0 \tag{5a}$$

$$u\frac{\partial u}{\partial x} - \frac{1}{\lambda^2}\frac{\partial^2 u}{\partial \zeta^2} + \left(h - \frac{\lambda'}{\lambda}\zeta u - \frac{1}{\lambda^2\zeta}\right)\frac{\partial u}{\partial \zeta} = \frac{\lambda'}{\lambda^3}\frac{k^2}{\zeta^2} - \frac{\partial P}{\partial x} \tag{5b}$$

$$\frac{\partial P}{\partial \zeta} = \frac{k^2}{\lambda^2\zeta^3} \tag{5c}$$

$$\frac{\partial}{\partial \zeta}(\zeta h) = -\zeta\frac{\partial u}{\partial x} + \frac{\lambda'}{\lambda}\zeta^2\frac{\partial u}{\partial \zeta} \tag{5d}$$

where $\lambda' \equiv d\lambda/dx$, and (5c) has been used to eliminate $\partial P/\partial\zeta$ in deriving (5b).

The initial conditions at $x = x_i$ are

$$k = k_i(\zeta)\,, \qquad u = u_i(\zeta)\,, \tag{6}$$

where the functions may be arbitrarily specified provided they satisfy the boundary conditions below and are consistent with the assumptions made in the previous section in deriving the basic equations.

The boundary conditions at the axis $\zeta = 0$ are

$$k = \frac{\partial u}{\partial \zeta} = h = 0 . \tag{7}$$

The boundary conditions on the outer bounding surface $\zeta = \zeta_b$ are

$$k = k_b(x), \qquad u = u_b(x), \qquad P = P_b(x), \tag{8}$$

and these, together with the shape $\lambda(x)$, may be arbitrarily specified; but if it is specified that ζ_b is a stream (or solid) surface a relation between the quantities is implied and they cannot be arbitrarily specified. If ζ_b is a stream surface then, by definition,

$$h_b/u_b = \zeta_b \lambda'/\lambda ,$$

so, if the shape $\lambda(x)$ of the boundary is given, the additional specification of u_b would make the problem overdetermined, since the differential equations (5) contain only a first derivative of h with respect to ζ. In general, here, only one of u_b and λ can be arbitrarily specified in addition to k_b and P_b. Still more is implied if the stream surface is inviscid with negligible diffusion across it, for equation (5a) then yields

$$k_b(x) = k_b(x_i) = \text{const} ,$$

and (5b) reduces to

$$u_b \frac{du_b}{dx} = \frac{\lambda'}{\lambda^3} \frac{k_b^2}{\zeta_b^2} - \frac{dP_b}{dx} ,$$

so that k_b is fixed by the initial conditions, and the additional specification of P_b and either u_b or λ automatically implies the specification of both u_b and λ, which would again make the problem overdetermined. Here only one of P_b, u_b and λ can be arbitrarily specified.

If ζ_b is a stream surface it is necessary to incorporate an iterative cycle into the computation to obtain a solution in which $h_b(x)$ takes values appropriate for a stream surface, namely values which satisfy the condition $h_b/u_b = \zeta_b \lambda'/\lambda$. Similarly if ζ_b is a solid surface then $k_b = u_b = 0$ and only one of P_b and λ can be arbitrarily specified, and a modification is required to ensure that $h_b = 0$.

4. *The Difference Equations and the Method of Solution.*

4.1. *The Difference Approximations.*

The calculation proceeds by marching in the direction of increasing x in steps δx. For each step the differential equations (5) are replaced by a set of difference equations covering the range $0 \geqslant \zeta \geqslant \zeta_b$, which is divided by pivotal points into N equal intervals $\delta\zeta$. To denote position a double-suffix notation is employed; thus $k_{m,n}$ denotes the value of k at the mth step and the nth pivotal point from the axis. For the present implicit method the approximations adopted are

$$
\left.
\begin{aligned}
k_{m+\frac{1}{2},n} &= \frac{1}{2}(k_{m+1,n}+k_{m,n}) \\
\left(\frac{\partial k}{\partial x}\right)_{m+\frac{1}{2},n} &\quad \frac{1}{\delta x}(k_{m+1,n}-k_{m,n}) \\
\left(\frac{\partial k}{\partial \zeta}\right)_{m+\frac{1}{2},n} &= \frac{1}{4\delta\zeta}(k_{m+1,n+1}-k_{m+1,n-1}+k_{m,n+1}-k_{m,n-1}) \\
\left(\frac{\partial^2 k}{\partial \zeta^2}\right)_{m+\frac{1}{2},n} &= \frac{1}{2(\delta\zeta)^2}(k_{m+1,n+1}-2k_{m+1,n}+k_{m+1,n-1}+k_{m,n+1}-2k_{m,n}+k_{m,n-1}).
\end{aligned}
\right\} \tag{9}
$$

Substitution of these, and of similar approximation for u, h and P, in the differential equations (5) yields for the $(m+1)$th step and the nth pivotal point the difference equations for k, u, P and h, where the equations are evaluated at $(m+\frac{1}{2},n)$, $(m+\frac{1}{2},n)$, $(m+1,n+\frac{1}{2})$ and $(m+\frac{1}{2},n-\frac{1}{2})$, respectively. The resulting equations are written in a form suitable for dealing with their non-linearity. In particular, the non-linear terms $u\partial u/\partial x$ and $u\partial u/\partial\zeta$ in equation (5b) are replaced by Newtonian approximations: the equation for the former, for example, being

$$
u_{m+\frac{1}{2},n}\left(\frac{\partial u}{\partial x}\right)_{m+\frac{1}{2},n} = \frac{u_{m+1,n}}{\delta x}(u_{m+1,n}) - \frac{u^2_{m+1,n}}{2\delta x} - \frac{u^2_{m,n}}{2\delta x},
$$

where the only term on the right-hand side that is treated as unknown is the one in brackets, the remainder being treated as given by the preceding cycle of an iteration.

4.2. *The Basic Difference Equations.*

For the case where the boundary surface of revolution is neither a stream nor a solid surface the resulting equations are

$$
a_n k_{m+1,n+1} + b_n k_{m+1,n} + c_n k_{m+1,n-1} = d_n, \tag{10a}
$$

where

$$
a_n = \frac{h_{m+\frac{1}{2},n}}{4\delta\zeta} - \frac{n(\lambda_{m+1}-\lambda_m)}{4\delta x(\lambda_{m+1}+\lambda_m)}(u_{m+1,n}+u_{m,n}) + \frac{1-2n}{n(\delta\zeta)^2(\lambda_{m+1}+\lambda_m)^2}
$$

$$
b_n = \frac{1}{2\delta x}(u_{m+1,n}+u_{m,n}) + \frac{4}{(\delta\zeta)^2(\lambda_{m+1}+\lambda_m)^2}
$$

$$
c_n = -a_n - \frac{4}{(\delta\zeta)^2(\lambda_{m+1}+\lambda_m)^2}
$$

$$
d_n = \frac{k_{m,n}}{2\delta x}(u_{m+1,n}+u_{m,n}) + \frac{2}{(\delta\zeta)^2(\lambda_{m+1}+\lambda_m)^2}(k_{m,n+1}-2k_{m,n}+k_{m,n-1}) -
$$

$$
- \left[a_n + \frac{2}{(\delta\zeta)^2(\lambda_{m+1}+\lambda_m)^2}\right](k_{m,n+1}-k_{m,n-1}),
$$

$$
a^*_n u_{m+1,n+1} + b^*_n u_{m+1,n} + c^*_n u_{m+1,n-1} = d^*_n, \tag{10b}
$$

where $1 \geqslant n \geqslant N-1$ and

$$a_n^* = \frac{h_{m+\frac{1}{2},n}}{4\delta\zeta} - \frac{n(\lambda_{m+1}-\lambda_m)}{4\delta x(\lambda_{m+1}+\lambda_m)}(u_{m+1,n}+u_{m,n}) - \frac{1+2n}{n(\delta\zeta)^2(\lambda_{m+1}+\lambda_m)^2}$$

$$b_n^* = \frac{u_{m+1,n}}{\delta x} + \frac{4}{(\delta\zeta)^2(\lambda_{m+1}+\lambda_m)^2} -$$

$$- \frac{n(\lambda_{m+1}-\lambda_m)}{4\delta x(\lambda_{m+1}+\lambda_m)}(u_{m+1,n+1}-u_{m+1,n-1}+u_{m,n+1}-u_{m,n-1})$$

$$c_n^* = -a_n^* - \frac{4}{(\delta\zeta)^2(\lambda_{m+1}+\lambda_m)^2}$$

$$d_n^* = \frac{1}{2\delta x}(u_{m+1,n}^2+u_{m,n}^2) - \frac{4(u_{m,n}-u_{m,n-1})}{(\delta\zeta)^2(\lambda_{m+1}+\lambda_m)^2} - a_n^*(u_{m,n+1}-u_{m,n-1}) -$$

$$- \frac{n(\lambda_{m+1}-\lambda_m)}{4\delta x(\lambda_{m+1}+\lambda_m)}(u_{m+1,n+1}-u_{m+1,n-1}+u_{m,n+1}-u_{m,n-1})\,u_{m+1,n} +$$

$$+ \frac{2(\lambda_{m+1}-\lambda_m)}{n^2\delta x(\delta\zeta)^2(\lambda_{m+1}+\lambda_m)^3}(k_{m+1,n}+k_{m,n})^2 - \frac{1}{\delta x}(P_{m+1,n}-P_{m,n}).$$

$$P_{m+1,n} = P_{m+1,n+1} - \frac{(k_{m+1,n+1}+k_{m+1,n})^2}{4(n+\frac{1}{2})^3(\delta\zeta)^2\lambda_{m+1}^2} \tag{10c}$$

$$h_{m+\frac{1}{2},n} = \left(1-\frac{1}{n}\right)h_{m+\frac{1}{2},n-1} \frac{(1-\frac{1}{2n})\delta\zeta}{2\delta x}(u_{m+1,n}-u_{m,n}+u_{m+1,n-1}-u_{m,n-1}) +$$

$$+ \frac{(n-\frac{1}{2})^2}{n}\frac{\delta\zeta}{\delta x}\frac{(\lambda_{m+1}-\lambda_m)}{\lambda_{m+1}+\lambda_m}(u_{m+1,n}-u_{m+1,n-1}+u_{m,n}-u_{m,n-1}). \tag{10d}$$

Since equation (10b) becomes meaningless, as it stands, at $\zeta = 0$, $n = 0$, a special form is used there, derived by use of the boundary conditions at $\zeta = 0$, where the expressions for a^*, b*, c^* and d^* are

$$\left.\begin{aligned} a_0^* &= -\frac{8}{(\delta\zeta)^2(\lambda_{m+1}+\lambda_m)^2} \\ b_0^* &= \frac{u_{m+1,0}}{\delta x} - a_0^* \\ c_0^* &= 0 \\ d_0^* &= \frac{u_{m,0}}{2\delta x}(u_{m+1,0}^2+u_{m,0}^2) - a_0^*(u_{m,1}-u_{m,0}) - \frac{1}{\delta x}(P_{m+1,0}-P_{m,0}) \end{aligned}\right\} \tag{10e}$$

4.3. *The Basic Cycle of Computations.*

If we put $n = 0, 1, 2, \ldots, N-1$ where $N = (\zeta_b/\delta\zeta)$ in equations (10) we obtain a set of difference equations which are to be solved in advancing from m to $m+1$. As the equations stand, however, they are non-linear and moreover cannot be solved separately. The interative procedure adopted here to deal with the non-linearity also enables the equations (10a) and (10b) to be solved successively for k and u, if use is made of equations (10c) and (10d) for P and h. The procedure may be followed in the diagram of Fig. 1, which represents the computer programme schematically, both for the present simpler cases in which the surface of revolution on which the outer boundary conditions are given is neither a stream nor a solid surface, and for the cases to be considered later in which this surface is either a stream or a solid surface.

The set of equations (10a) for k is solved first. The quantities $h_{m+\frac{1}{2},n}$ and $u_{m+1,n}$ that occur in the coefficients a_n, b_n, c_n and d_n are assigned values obtained in the previous cycle in the iteration. For the first cycle the assigned values are obtained by extrapolation from the previous step. The set of equations (10a) is thus rendered linear and can be solved simultaneously independently of equations (10b), (10c) and (10d) to yield $k_{m+1,n}$ for $n = 1, 2, \ldots, N-1$. The method of solution will be outlined below after the complete cycle has been described. The set of equations (10b) is solved next. The quantities $k_{m+1,n}$ are known from the solution of (10a). The equations (10c) give $P_{m+1,n}$. The quantities $h_{m+\frac{1}{2},n}$ and $u_{m+1,n}$ that occur in the coefficients a_n^*, b_n^*, c_n^* and d_n^* are assigned values obtained in the previous cycle. The set (10b) can then be solved simultaneously to yield $u_{m+1,n}$ for $n = 0, 1, 2, \ldots, N-1$. The cycle is then completed by substituting the values of $u_{m+1,n}$ in the equations (10d) to evaluate $h_{m+\frac{1}{2},n}$. The cycles are repeated until successive values agree, that is, differ by less than some prescribed small amount, and the calculation then proceeds to the next step.

Both equations (10a) and equations (10b) are solved by triangular resolution of the matrix and back-substitution. It suffices to describe a solution of (10a) for k. In this equation a_n, b_n, c_n and d_n are known expressions. Note that, for $n = N-1$, $k_{m+1,n+1}$ is a specified boundary condition so that in this case the first term $a_n k_{m+1,n+1}$ is transferred to the right-hand side of the equation. In matrix form equations (10a) can be written

$$AK = D\,, \tag{11}$$

where A is an $(N-1)\times(N-1)$ square matrix and K and D are column vectors. The procedure is to resolve A into lower and upper triangular matrices, $A = LU$, where both L and U have non-zero elements in only the main and an adjoining diagonal; then put $LY = D$ and evaluate Y; and finally put $UK = Y$ and evaluate K. Thus it is found that, if the terms in the main diagonal of U are denoted by U_n, and those in Y by y_n,

$$\left.\begin{aligned} n = N-1, &\qquad U_n = b_n\,, \\ n = N-2, N-3, \ldots, 1, &\qquad U_n = b_n - a_n c_{n+1}/U_{n+1}\,; \end{aligned}\right\} \tag{12}$$

$$\left.\begin{aligned} n = N-1, &\qquad y_n = d_n\,, \\ n = N-2, N-3, \ldots, 1, &\qquad y_n = d_n - a_n y_{n+1}/U_{n+1}\,; \end{aligned}\right\} \tag{13}$$

$$n = 1, 2, \ldots, N-1, \qquad k_n = (y_n - c_n k_{n-1})/U_n\,. \tag{14}$$

It can be seen that the calculation proceeds from the outside ($n = N-1$) inwards to evaluate U_n and y_n, and from the inside ($n = 1, k_{n-1} = 0$) outwards to evaluate k_n (that is, $k_{m+1,n}$).

When the surface of revolution on which the boundary conditions are given is a stream or solid surface the above procedure needs modification. The above numerical technique requires that $\lambda_{m+\frac{1}{2}}$, $k_{m,N}$, $u_{m,N}$ and $P_{m,N}$, that is λ, k_b, u_b and P_b respectively, be specified but, as pointed out earlier, such a specification here would make the problem overdetermined: the calculated value of $h_{m+\frac{1}{2},N}$ (that is, h_b)

would in general be incorrect. A procedure that may be adopted is to calculate, by the basic iteration described in section 4.3, $h_{m+\frac{1}{2},N}$ for two trial sets of boundary conditions and then to iterate by linear interpolation until the desired value of $h_{m+\frac{1}{2},N}$ is obtained. However, when the shape of the surface is specified, this outer iteration can be readily avoided by solving a more complicated set of equations. These two procedures will be considered in turn.

4.4. *An Outer Iteration.*

When the bounding surface of revolution is a stream surface across which there is no diffusion, we have seen that only one of the boundary values $u_b(x)$, $P_b(x)$ and $\lambda(x)$ can be arbitrarily specified ($k_b(x)$ is given by the initial conditions). But the conditions that must be satisfied on such a boundary are

$$\frac{h_b}{u_b} = \zeta_b \frac{\lambda'}{\lambda}$$

$$u_b \frac{du_b}{dx} = \frac{\lambda'}{\lambda^3} \frac{k_b^2}{\zeta_b^2} - \frac{dP_b}{dx}.$$

If one of the two unknown boundary values is somehow estimated, the latter equation yields the second, and the basic computation described above can be made to determine h_b. Successive estimates are made until the computed value of h_b satisfies the first equation $h_b/u_b = \zeta_b \lambda'/\lambda$. When the specified quantity is P_b or u_b it is the value of λ that is estimated and we write, for the $(m+1)$th step,

$$\lambda_{m+1} = \alpha_0[\lambda_m + (\lambda_m - \lambda_{m-1})],$$

so that it is the factor α_0 that is sought. The subscripts 0,–1,–2, are used to denote current and successive preceding values of a quantity in the succession of estimates. For the first estimate we put

$$\alpha_0 = 1 ;$$

for the second,

$$\alpha_0 = \frac{\lambda_m + \beta_0 \lambda_m \delta x/\zeta_b}{\lambda_m + (\lambda_m - \lambda_{m-1})},$$

where β_0 is the current value of h_b/u_b;
and for the following estimates we interpolate linearly by putting

$$\alpha_0 = \alpha_{-2} + \frac{(\beta_{-1} - \gamma_{-1})(\alpha_{-1} - \alpha_{-2})}{(\beta_{-1} - \gamma_{-1}) - (\beta_0 - \gamma_0)},$$

where γ_0 is the current value of $\zeta_b \lambda'/\lambda$, etc. A similar scheme may be followed when the specified quantity is λ, but here an alternative direct method, described in the next Section, is available.

When the bounding surface of revolution is a solid surface, we have seen that only one of the boundary values $P_b(x)$ and $\lambda(x)$ can be arbitrarily specified ($u_b = k_b = 0$). But the condition that must be satisfied on such a boundary is

$$h_b = 0 .$$

If the unknown value of P_b or λ is estimated, the basic computation can be made to determine h_b. Successive estimates are made until the computed value of h_b is zero. When the specified quantity is $P_b(x)$ we write

$$\lambda_{m+1} = \alpha_0[\lambda_m + (\lambda_m - \lambda_{m-1})]$$

as before, and for the successive estimates put

(i) $$\alpha_0 = 1 \ ;$$

(ii) $$\alpha_0 = \frac{2\left[\left(\frac{\partial^2 u}{\partial \zeta^2}+\frac{1}{\zeta}\frac{\partial u}{\partial \zeta}\right)_b \Big/ \frac{dP_b}{dx}\right]^{\frac{1}{2}} - \lambda_m}{\lambda_m+(\lambda_m-\lambda_{m-1})},$$

which is suggested by the boundary condition

$$\frac{dP_b}{dx} = \frac{1}{\lambda^2}\left(\frac{\partial^2 u}{\partial \zeta^2}+\frac{1}{\zeta}\frac{\partial u}{\partial \zeta}\right)_b;$$

(iii) $$\alpha_0 = \alpha_{-2}+\frac{\beta_{-1}(\alpha_{-1}-\alpha_{-2})}{\beta_{-1}-\beta_0},$$

where β_{-1}, β_0 are now successive values of h_b. Again, a similar scheme may be followed when the specified quantity is $\lambda(x)$, but the direct method given below is preferred.

4.5. *A Procedure for Cases of Specified Boundary Shape.*

It has been noted that when the surface of revolution on which the boundary conditions are given is a stream or solid surface of specified shape no outer iteration is needed. Although the basic cycle of computations outlined in section 4.3 suffices, the details are more complicated.

Consider first the case of a specified bounding stream surface ζ_b with negligible diffusion across it. On this surface the velocity components and the pressure are related (*see* Section 3) by the equations

$$\left.\begin{aligned} h_b/u_b &= \zeta_b \lambda'/\lambda \\ u_b\frac{du_b}{dx} &= \frac{\lambda'}{\lambda^3}\frac{k_b^2}{\zeta_b^2} - \frac{dP_b}{dx} \\ k_b &= \text{const.} \end{aligned}\right\} \tag{15}$$

Since $\lambda(x)$ is specified and k_b is given by the initial conditions the values of h_b, u_b and P_b must be left unspecified; they should emerge in the course of the solution.

In the procedure adopted here u_b is regarded as an unknown, and the equation required to make u_b determinate is derived by integrating the continuity equation (5d) for h_b and substituting in the first of the equations (15) above. The required equation is,

$$u_b = \frac{\lambda}{\lambda'\zeta_b^2}\int_0^{\zeta_b}\left(-\zeta\frac{\partial u}{\partial x}+\frac{\lambda'}{\lambda}\zeta^2\frac{\partial u}{\partial \zeta}\right)d\zeta \tag{16}$$

The pressure P is eliminated from the differential equations to be solved by making use of the second of equations (15), and also the equation (5c), to obtain

$$\frac{\partial P}{\partial x} = \frac{\lambda'}{\lambda^3}\frac{k_b^2}{\zeta_b^2} - u_b\frac{du_b}{dx}+\frac{\partial}{\partial x}\left[\int_{\zeta_b}^{\zeta}\frac{k^2}{\lambda^2\zeta^3}d\zeta\right].$$

Thus, if we substitute this expression for $\partial P/\partial x$ into equation (5b), we have three differential equations, (5a), (5b) and (5d), and the equation (16), to be solved simultaneously.

The corresponding difference equations are derived by substituting difference approximations as before and by replacing the integrals by sums. The equations for k are unchanged; they are

$$a_n k_{m+1,n+1} + b_n k_{m+1,n} + c_n k_{m+1,n-1} = d_n, \tag{17a}$$

where $1 \leqslant n \leqslant N-1$ and the a_n, b_n, c_n and d_n are the same as given below equation (10a) in Section 4.2. For u, however,

$$a_n^* u_{m+1,n+1} + b_n^* u_{m+1,n} + c_n^* u_{m+1,n-1} + \alpha_{n,-1} u_{m+1,N} = d_n^{**} \tag{17b}$$

where $1 \leqslant n \leqslant N-1$ and the a_n^*, b_n^* and c_n^* are the same as given below equation (10b) in Section 4.2, but

$$d_n^{**} = \left[d_n^* + \frac{1}{\delta x}\left(P_{m+1,n} - P_{m,n}\right) \right] - \frac{1}{2\delta x}(u_{m+1,N}^2 + u_{m,N}^2) -$$

$$- \frac{2(\lambda_{m+1} - \lambda_m)}{N^2\, \delta x\, (\delta\zeta)^2\, (\lambda_{m+1} + \lambda_m)^3} (k_{m+1,N} + k_{m,N})^2 +$$

$$+ \frac{1}{4\delta x\, (\delta\zeta)^2} \sum_n^N \frac{1}{(n+\frac{1}{2})^3} \left[\frac{1}{\lambda_{m+1}^2} (k_{m+1,n+1} + k_{m+1,n})^2 - \right.$$

$$\left. - \frac{1}{\lambda_m^2} (k_{m,n+1} + k_{m,n})^2 \right]$$

and

$$\alpha_{n,-1} = -\frac{u_{m+1,N}}{\delta x}$$

for $1 \leqslant n \leqslant N-1$.

As before, a special form of (17b) is needed at $n = 0$. The coefficients a_0^*, b_0^* and c_0^* are the same as those given in (10e), $\alpha_{0,-1} = \alpha_{n,-1}$, and d_0^{**} is given by the general expression for d_n^{**} above, with d_0^* given by (10e). To be solved simultaneously with (17b) is the difference form of equation (16), namely

$$\sum_0^N \beta_{-1,n}\, u_{m+1,n} = \gamma \tag{17c}$$

where

$$\beta_{-1,0} = -\tfrac{1}{2}\lambda_{m+1},$$

$$\beta_{-1,n} = -n(3\lambda_{m+1} - \lambda_m)$$

for $1 \leqslant n \leqslant N-1$,

$$\beta_{-1,N} = -\tfrac{1}{2}[(3N-1)\,\lambda_{m+1} - N\lambda_m]$$

and
$$\gamma = -\tfrac{1}{2}\lambda_m u_{m,0} + \sum_{n=1}^{N-1} n(\lambda_{m+1} - 3\lambda_m) u_{m,n} +$$
$$+\tfrac{1}{2}[N\lambda_{m+1} - (3N-1)\lambda_m] u_{m,N}$$

The set of difference equations is completed by the continuity equation, identical to (10d), which yields h from u.

The cycle of computations is basically the same as that described in Section 4.3 and illustrated in Fig. 1. The equations (17a), and the combination of (17b) and (17c), are solved by triangular resolution of the matrix and back-substitution.

The case of a solid specified bounding surface ζ_b may be treated similarly. On this surface

$$\left.\begin{aligned} k_b = u_b = h_b = 0 \\ \frac{1}{\lambda^2}\frac{\partial^2 u}{\partial \zeta^2} + \frac{1}{\lambda^2 \zeta}\frac{\partial u}{\partial \zeta} = \frac{dP_b}{dx} \end{aligned}\right\} \tag{18}$$

Since $\lambda(x)$ is specified the value of P_b must be left unspecified. In the procedure adopted for this case P_b is regarded as an unknown in the difference approximations to the equation (5b) for u. The additional equation required to make the system determinate is derived by integrating the continuity equation (5d) for h_b and setting $h_b = 0$. It is

$$\int_0^{\zeta_b} \left(-\zeta \frac{\partial u}{\partial x} + \frac{\lambda'}{\lambda}\zeta^2 \frac{\partial u}{\partial \zeta}\right) d\zeta = 0 .$$

The difference equations are the same as above, except that instead of (17b) there is

$$a_n^* u_{m+1,n+1} + b_n^* u_{m+1,n} + c_n^* u_{m+1,n-1} + \frac{1}{\delta x} P_{m+1,N} = d_n^{***} \tag{19}$$

with
$$d_n^{***} = \left[d_n^* + \frac{1}{\delta x} P_{m+1,n}\right] .$$

5. *Examples.*

5.1. *General Features of the Computations.*

To illustrate the application of the method under a variety of conditions three different examples are given below. The computations were carried out on a Mercury digital computer using a programme in Autocode. A corresponding programme could be written for any digital computer of moderate capacity. The limited capacity of Mercury makes care necessary in the detailed layout of the programme when the minimum interval in the radial direction is sought. A maximum of about 90 intervals (or pivotal points) can be handled here without venturing beyond the high-speed store; for 80 intervals the basic cycle of computations occupied the Mercury computer for 15 sec. The total time for a computation depends also on the number of iterations required at each step and on the number of steps; for the present examples it was found to be roughly in direct proportion to the number of intervals $\delta\zeta$ and the number of steps δx.

The procedure in beginning a computation differs slightly from that used to advance from one step to the next. In the latter case values are extrapolated from the previous step for the first cycle of an iterative sequence. For the first cycle of the first step this is not possible and specified initial values are substituted.

The choice of the step size δx is a compromise. The step chosen should be small enough for the truncation errors involved to be acceptable, and yet it should not be so small that the time for the computation, which is roughly proportional to the number of steps, becomes excessive. Since the truncation errors depend on the x-wise variations of k, u, etc., the choice of step size δx may be guided by the x-wise variations in the boundary conditions and by information obtained in the earlier, upstream, stages of the computation. Another consideration is the requirement that the iterations converge; reduction of step size usually promotes convergence.

The accuracy of the computed results can be improved by repeating the computation with different intervals $\delta\zeta$ and using standard methods for extrapolating to the limit $\delta\zeta \to 0$. For example, in the method used here it is assumed, since first-order central differences are employed, that a more accurate value of u is given by the expansion

$$u = u_{comp} + B(\delta\zeta)^2 + C(\delta\zeta)^4 + \ldots ,$$

where u_{comp} is the computed value for the interval $\delta\zeta$, and B, C, ... , are constants. Thus if the computation is carried out for three different intervals, substitution in the above expansion yields three equations from which, u, B and C can be determined, and the error in u associated with $\delta\zeta$ would be of the order $(\delta\zeta)^6$.

The examples that follow relate to fluid motions of types that actually occur; at the same time the examples illustrate the three main variants in the application of the method : where the bounding surface of revolution is neither a stream nor a solid surface, where it is a stream surface, and where it is a solid surface. For each example a description is given of the initial and boundary conditions, the mesh sizes, the results and the time taken. Distinctive features of each example are commented upon.

5.2. *A Trailing Vortex*

This is the simplest of the three examples to be described, and for this case no study of the effects of different step sizes is made. The initial conditions here are taken to be

$$x = 0{\cdot}25 , \qquad u = 1 - 0{\cdot}25e^{-\zeta^2} , \qquad k = 0{\cdot}5 - 0{\cdot}5e^{-\zeta^2} \qquad (\equiv \zeta v) .$$

The simple forms for the profiles (shown in Figs. 2 and 3) were taken from the approximate theory of Newman[9]. Batchelor[10] has recently shown that while the form for k, or $v \equiv k/\zeta$. is correct in an asymptotic sense the correct asymptotic form for u includes extra terms involving the circulation around the vortex. Neither theory is strictly applicable here, because neither the circumferential velocity v, nor the defect of axial velocity $(1-u)$, is small compared with the axial velocity u. It is of interest, nevertheless, to check whether either theory gives results approaching those obtained numerically.

The outer bounding surface of the core is taken to be a circular cylinder (so that the shape factor $\lambda = 1$) with

$$\zeta_b \equiv Re^{\frac{1}{2}} r/\lambda = 6 ,$$

and the computation is carried downstream as far as $x = 1{\cdot}0$. The boundary conditions at $\zeta = 6$, for $0{\cdot}25 \geqslant x \geqslant 1{\cdot}0$ are taken to be

$$u = 1 , \qquad k = 0{\cdot}5 , \qquad P = const .$$

This is justified provided viscous effects do not extend outside $\zeta = 6$, and the computation confirms the point.

The computation follows the simpler procedure outlined in Section 4.3. The step sizes are

$$\delta x = 0{\cdot}05 , \qquad \delta\zeta = 0{\cdot}075 ,$$

so that there are 15 x-wise steps taken and 80 intervals in the radial direction. The number of cycles required (for successive values of u on the axis to differ by less than 10^{-5}) range from 6 for the first step to 3 for the middle steps and 2 for the last few steps. The time taken by the computer (Mercury) for the whole computation is 12 minutes.

Computed profiles of the axial velocity u and the circumferential velocity v are shown in Figs. 2 and 3 respectively. The values are plotted against the non-dimensional variable $R \equiv Re^{\frac{1}{2}}r$ so that different values of the scaling quantities q, l and ν are automatically allowed for. Also plotted in Fig. 2 is the profile that Newman's solution gives at $x = 1{\cdot}0$; it shows a much more marked increase in axial velocity with increasing distance downstream than is given by the numerical solution. This discrepancy is the net result of an augmentation of velocity (in Newman's case), due to Newman's neglect of the pressure-gradient term in the equation of motion (3b), and a reduction of velocity due to Newman's linearization of the equations of motion. It can be checked that Batchelor's solution provides no better fit to the numerical results; in his case the increase in axial velocity with distance downstream is less marked than the numerical increase because the only contribution to the discrepancy comes from the linearization of the equations of motion. On the other hand the linear theories are found to give results for the circumferential velocity which are almost identical to those obtained numerically. The profiles of Newman and Batchelor are identical here and two of them are shown in Fig. 3.

It may be noted that the numerical solution is valid for any values of the scaling quantities q, l and ν provided the quasi-cylindrical approximation is nowhere invalidated, in particular, provided $ql/\nu \gg 1$. For example, if we choose $\nu = 0{\cdot}3$ ft^2/sec and $rlvq \to 240$ ft^2/*sec* for increasingly large rl (typical values for a turbulent trailing vortex far behind an actual aircraft), then, since $\zeta v \to 0{\cdot}5$ here, $ql = 768\,000$; so $ql/\nu = 2{\cdot}56 \times 10^6$, and if we choose $q = 320$ *ft/sec* (so that $u\,q$ also takes a typical value) we find $l = 2400$ *ft*. The range $0{\cdot}25 \leqslant x \leqslant 1{\cdot}0$ then covers a distance of 1800 ft. A single numerical solution thus covers a whole range of actual flows.

5.3. *The Core of a Leading-edge Vortex.*

The vortex core considered in this example is of the type that might actually occur in the separated flow over a delta wing. Upstream, the outer inviscid part of the core is taken to be conical. Further downstream the outer flow field gradually departs from the conical state, accompanied by a rise in pressure of a magnitude that might be appropriate for the effect of the trailing edge of the wing. As might be expected there is a substantial decrease in the velocity along the axis, but in this example no stagnation occurs.

The computation falls naturally into two parts, corresponding to the upstream and downstream parts of the flow. For the first part the outer bounding surface of the core is taken to be conical, and the simple computation procedure outlined in Section 4.3 and used for the numerical solution for the trailing vortex in the previous Sub-section is used. For the second part the outer bounding surface of the core is taken to be a stream surface of unspecified shape but with a specified pressure distribution along it. The computation then includes the outer iteration described in Section 4.4. The first part of the computation provides initial conditions for the second part.

The initial conditions, for the upstream part of the flow, are assumed to be given, at $x = 50$, by the solution of Stewartson and Hall[3] for the core of a leading-edge vortex. The initial profiles of u and v, derived from the authors' tables, are shown in Figs. 4 and 5 respectively. The radius of the bounding cone, at $x = 50$, was $R_b = 9{\cdot}6295$ (so that $\zeta_b = 9{\cdot}6295$) and the cone was supposed to extend to $x = 100$ where $R_b = 19{\cdot}259$; on this cone the velocity and pressure were assumed to be constant.

The computed profiles of axial and circumferential velocity at $X = 100$ are shown in Figs. 4 and 5. For this part of the computation the step sizes are $\delta x = 5$ and $\delta\zeta = 0{\cdot}120369$, so that 10 steps are required in the x-direction and there are 80 intervals in the radial direction. No checks with different step sizes are made, because the main object is to obtain a set of initial conditions for the second part of the computation. However, the results may be compared with those given by the theory of Stewartson and Hall, even though the boundary conditions assumed here are not precisely the same as those appropriate to the theory, which requires a slight increase in both axial and circumferential velocity with increasing

distance x along the cone. The discrepancy (0·5 per cent) between the theory and the computed results is no more than the discrepancies in the boundary conditions. This part of the computation is completed in about 10 minutes by the Mercury computer when iteration is continued till successive values of u on the axis differ by less than 10^{-2}.

The second part of the computation is concerned with the structure of the flow within the stream tube passing through $R_b = 19{\cdot}259$ at $x = 100$, from $x = 100$ to $x = 140$. It is assumed that there is no diffusion across the stream tube. The prescribed pressure distribution along this bounding stream-tube is shown in Fig. 6, which also shows the radius of the tube determined in the course of the computation. The computation may be regarded as a numerical experiment to study the effect of an arbitrarily imposed pressure gradient on a given vortex core. Formally, the initial conditions, for this part of the computation are

$$x = 100 , \qquad u = u(\zeta)$$
$$k = k(\zeta)$$

given by the preliminary computation; and the boundary conditions at $\zeta_o = 9{\cdot}6295$ are

$$\frac{h_b}{u_b} = \zeta_b \frac{\lambda'}{\lambda} ,$$

$$u_b \frac{du_b}{dx} = \frac{\lambda'}{\lambda^3} \frac{k_b^2}{\zeta_b^2} - \frac{dP_b}{dx} ,$$

$$k_b = 40{\cdot}4064 ,$$

$$P_b = P_b(x) ,$$

where P_b is specified as the function shown in Fig. 6 and is a smooth but otherwise arbitrary continuation of conditions at $x = 100$. This is an example in which successive estimates of the value of λ are made in the manner described in Section 4·4. The computation is carried out for a range of step sizes:

$$\delta x = 2(20) ; \qquad \delta\zeta = 0{\cdot}120369(80) , \qquad 0{\cdot}240738(40) , \qquad 0{\cdot}481475(20) ;$$

and

$$\delta x = 1(40) ; \qquad \delta\zeta = 0{\cdot}240738(40) .$$

For the case $\delta x = 2$, $\delta\zeta = 0{\cdot}120369(80)$, the time taken by the Mercury computer to compute the solution from $x = 100$ to $x = 140$ is about 75 minutes.

Some results for the case $\delta x = 2$, $\delta\zeta = 0{\cdot}120369$, are shown in Figs. 4, 5 and 6. In Figs. 4 and 5 are shown profiles of the axial and circumferential velocity, respectively, at $x = 124$ and $x = 140$. Fig. 6 shows the computed variation of radius $R_b = \zeta_b\lambda$ from $x = 100$ to $x = 140$. The effect of mesh size on the computed values of u, v and R_b is shown in Table 1. There are four columns of computed results, and one column obtained by extrapolation from columns 1, 3 and 4 by the method described in Section 5.1. In column 2 are results computed with the step size δx equal to half that used for column 3, but with the same value of $\delta\zeta$ as for column 3. As expected for such an implicit method of calculation, there is no sign of numerical instability. The effect on u of halving the step-size in the x-direction is less than the error (0·01) due to terminating the iteration after a finite number of cycles. The truncation errors due to the finite size of the interval $\delta\zeta$ may be estimated by comparing the computed results with the extrapolated values. The truncation errors are seen to be appreciable (~ 1 per cent) for the largest interval, but they are much smaller ($\sim 0{\cdot}1$ per cent) with the smallest interval.

As with the previous example, the numerical solution is valid for a whole range of the scaling quantities, q, l and ν. For example, if we choose $q = 1$ ft/sec, $l = 1$ ft and $\nu = 0{\cdot}0008$ ft^2/sec, we have $ql/\nu = 1{\cdot}25 \times 10^5$ which satisfies the condition $ql/\nu \gg 1$; then, over a distance of 40 ft, the axial velocity on the axis decreases from about 680 ft/sec to about 430 ft/sec, the maximum value of the circumferential velocity decreases from about 240 ft/sec to 200 ft/sec and the core itself expands from a diameter of about 1·1 ft to about 1·5 ft.

5.4. *A Vortex in a Pipe*

The pipe-flow considered here has the same initial conditions as the one chosen by Abbott[4] for study. The pipe itself is prescribed to be a circular cylinder, and the initial conditions, at $x = 0$, are

$$u = 20 + 4\zeta^2 - 1{\cdot}6\zeta^4$$

$$k = 4\zeta^2(\sqrt{5} - \zeta) ,$$

with $\zeta = \sqrt{5}$ at the cylinder wall, that is, $\zeta_b = 2{\cdot}23607$. On the cylinder wall $u = 0$, $k = 0$ and $\lambda = 1$. This is an example in which successive estimates of the value of pressure at the wall, P_o, are made in the manner described in Section 4.5. No fair comparison with Abbotts' results can be made because his basic differential equations differ from the equations used here.

The initial profiles of axial velocity u and circumferential velocity v, and computed profiles for different stations in the range $0 < x \leqslant 75$, are shown in Figs. 7 and 8. The corresponding computed pressure distribution along the wall is shown in Fig. 9. For this computation the intervals $\delta\zeta$ in the radial direction are constant, that is

$$\delta\zeta = 0{\cdot}0559017(40) ,$$

but the step-sizes δx are increased with increasing distance downstream, with successive magnitudes

$$\delta x = 0{\cdot}3125(4), \quad 0{\cdot}625(2), \quad 1{\cdot}25(2), \quad 2{\cdot}5(4), \quad 5(4), \quad 10(4) .$$

The time taken by the Mercury computer is about 120 minutes. It can be seen from Figs. 7 and 8 that the computed flow tends to the known Hagen-Poiseuille state, with no swirl and a parabolic velocity profile, with increasing distance downstream. Moreover, Fig. 9 shows that the computed pressure gradient on the wall also tends to the Hagen-Poiseuille value. This is a check on the computation. A further check can be made by repeating the computation with larger intervals $\delta\zeta$. Typical results for u, v and P are shown in Table 2. Again there are four columns of computed results and one column obtained by extrapolation from columns 1, 3 and 4. The computation of the results in column 2 differed from that for the results in 3 only in that larger steps δx were used. Also included are a few values of u and dP/dx, appropriate for the Hagen-Poiseuille flow with the same value of mass-flow as the computed pipe-flow. The results clearly tend to some limit with decreasing interval. We may estimate the limiting values by assuming, as in the previous Section, that the errors depend on the squares and fourth powers of the interval; and the table shows that the extrapolated values downstream approach the Hagen-Poiseuille values closely.

At the larger x-wise steps the computations show a feature worth noting. If the computed values near the pipe-wall of either the axial or the circumferential velocity component are plotted as the computation proceeds downstream, the points are found to lie not on a smooth curve but rather on a wavy one. This is most marked in the upstream part where the axial gradients are larger. Such a plot (among others) is shown in Fig. 10; the points denoted by a small square are obtained in the case of the largest steps—where the first step is $\delta x_i = 2{\cdot}5$. All the plots in the Figure are for the computed values of the axial velocity u at a distance of one-tenth of the pipe-radius from the wall. The figure shows the virtual elimination of the oscillatory behaviour when the x-wise steps are reduced in size, whether the radial intervals $\delta\zeta$ are large or small, and this means that it is the truncation errors in the finite-difference approximations to the x-derivatives, or the errors introduced by replacing each ζ-derivative at the mid-point of an interval δx by the mean of its values at the end points of the interval, that are responsible for the oscillations.

Again we may assign a range of physical magnitudes to the computed flow. If, for example, the radius of the pipe is 10 cm, $q = 10$ cm/sec, and $\nu = 0{\cdot}2$ cm^2/sec, then, since

$$\zeta_b = r_b(ql/\nu)^{\frac{1}{2}} = \sqrt{5},$$

$$l = 1000 \text{ cm}$$

and

$$\frac{ql}{\nu} = 5 \times 10^4 ;$$

and we can say that in a distance of about 10 metres the velocity along the axis has increased from 200 cm/sec to about 95 per cent of its ultimate value of $333\frac{1}{3}$ cm/sec for downstream, and the maximum value of the circumferential velocity in a section has decreased to about 16·5 cm/sec, or one-third of its initial value of 50 cm/sec.

6. *Discussion.*

A numerical method for solving the equations for quasi-cylindrical vortex cores has been described, and the use of the method has been illustrated with three distinct examples. The examples show that the method is straightforward to apply and is numerically stable, and that only moderate times are required by a digital computer of relatively small capacity. The examples also illustrate practical purposes for which the method may be useful: each example relates to a fluid motion of a type that actually occurs and in circumstances of practical interest; and it seems that in no case can a solution be obtained analytically. Finally, it is found that the iterations converge when there are two velocity components just as when there is only one (as in a two-dimensional boundary layer).

The method is now being applied to a fluid motion in which "vortex breakdown" (*see* for example Ref. 1) occurs. Now a characteristic of this phenomenon is the presence of a free stagnation point and, of course, the method becomes invalid as stagnation is approached, because the axial gradients then become large enough to invalidate the quasi-cylindrical approximation, just as the boundary-layer approximation becomes invalid as separation is approached. But it seems fair to expect, as is done in boundary-layer calculations, that the behaviour of the solution will betray the imminence of stagnation even if a zero value of the axial velocity is not actually obtained. If this is so, the method may provide a means of predicting whether breakdown will occur in a given vortex core subject to given constraints, and also a means, by numerical experiment, of identifying and studying the conditions which favour or inhibit. In the case now being considered the bounding surface of revolution is a stream surface and the pressure along it (but not its shape) is prescribed; both this boundary condition and the upstream initial conditions are taken from experimental observations by Kirkpatrick[11] of a flow in which breakdown actually occurs.

The success of the present method suggests that similar methods might prove successful for related problems where the governing partial differential equations are of the parabolic type. An obvious example is provided by the compressible vortex core. Very recently Brown[12] obtained an analytic solution for an inviscid conical vortex core of the type associated with the separated flow over slender delta wings. The only viscous solutions available are certain similarity solutions (*see* for example Ref. 1) in which the freedom to prescribe initial and boundary conditions is lost. No other solutions are known to the present author. The current practical interest in such vortex cores makes it worth while to attempt to solve the governing equations numerically. The equations themselves are written down in Ref. 1; in addition to the continuity equation and three momentum equations, which are very similar to the equations (3), there is an energy equation and the equation of state, which enable the temperature and density to be determined in addition to the pressure and the velocity components. It seems that no large departure from the present method is needed: a straightforward extension should suffice.

LIST OF SYMBOLS

A	$(N-1)\times(N-1)$ square matrix
a, b	Units of step size; subscript b denotes conditions on outer bounding surface
a_n, b_n, c_n	Elements of the matrix A, coefficients in difference equations
$a_n^*, b_n^*, c_n^*, d_n^*, d_n^{**}, d_n^{***}$	Coefficients in difference equation (10b)
B, C	Constants
D	Column vector
d_n	Element of the column vector D, coefficient in difference equation
f_1, f_2	Values of the step δx
h	W/λ
i	Subscript denoting initial conditions on the upstream cross-section $x = x_i$
K	Column vector
k	$\lambda\zeta v$
k_n	Element of the column vector K
L	Lower triangular matrix
l	Reference length
m	Denotes mth step in axial direction
N	Total number of intervals $\delta\zeta$ in radial direction
n	Denotes nth pivotal point in radial direction
P	Non-dimensional pressure, actual pressure $\div$ ($q^2 \times$ density)
q, q_∞	Reference velocities
R	Radial ordinate, $Re^{\frac{1}{2}}r$
Re	Reference Reynolds number, ql/v
r	Non-dimensional radial ordinate, radial distance $\div$ l
U	Upper triangular matrix

u, v, w	Non-dimensional axial, circumferential and radial velocity components (actual velocity $\div q$)
W	$Re^{\frac{1}{2}}w$
x	Non-dimensional axial ordinate, axial distance $\div l$
Y	Column vector
y_n	Element of the column vector Y
$\alpha_{-2}, \alpha_{-1}, \alpha_o$ β_{-1}, β_o γ_{-1}, γ_o	Successive values used in iterative procedures of Section 4
$\alpha_{n,-1}$ $\beta_{-1,n}$ γ	Terms in difference equations of Section 4.5.
ζ	Radial ordinate, R/λ
λ	$r_b(x)/r_b(x_i)$
ν	Kinematic viscosity

REFERENCES

No.	Author(s)	Title, etc.
1	M. G. Hall	*The structure of concentrated vortex cores.* Progress in Aeronautical Sciences, Vol. 7, pp. 53–110. Pergamon Press (1966).
2	I. S. Gartshore	Some numerical solutions for the viscous core of an irrotational vortex. N.R.C. (Canada) LR–378. June, 1963.
3	K. Stewartson and M. G. Hall	The inner viscous solution for the core of a leading-edge vortex. *J. Fluid Mech., 15*, 306–318, 1963.
4	M. R. Abbott	Axially symmetric steady motion of a viscous incompressible fluid: some numerical experiments. R.A.E. Tech. Note No. Math 98, (A.R.C. 24,938). February, 1963.
5	D. R. Hartree	The solution of the equations of the laminar boundary layer for Schubauer's observed pressure distribution for an elliptic cylinder. A.R.C. R. & M. 2427. April, 1939.
6	D. C. Leigh	The laminar boundary-layer equation: a method of solution by means of an automatic computer. *Proc. Camb. Phil. Soc., 51*, 320, 1955.
7	R. M. Terrill	Laminar boundary-layer flow near separation with and without suction. *Phil. Trans.* A *253*, 55, 1960.
8	D. Catherall and K. W. Mangler	An indirect method for the solution of the Navier-Stokes equations for laminar incompressible flow at large Reynolds numbers. R.A.E. Rep. No. Aero 2683, (A.R.C. 25,599). October, 1963.
9	B. G. Newman	Flow in a viscous trailing vortex. *Aero. Quart. X*, 149–162, 1959.
10	G. K. Batchelor	Axial flow in trailing line vortices. *J. Fluid. Mech., 20*, 645–658, 1964.
11	D. L. I. Kirkpatrick ..	Experimental investigation of the breakdown of a vortex in a tube. A.R.C. C.P.821. May, 1964.
12	S. N. Brown	The compressible inviscid leading edge vortex. *J. Fluid Mech., 22*, 17–32, 1965.

TABLE 1

Effect of Mesh Size on Computed Values for a Leading-edge Vortex

$\delta x \propto a, \quad a = 2;$

$\delta \zeta \propto b, \quad b = 0{\cdot}120369.$

x	$\frac{R}{R_b}$	u				
		$\delta x = a, \delta\zeta = 4b$	$0{\cdot}5a, 2b$	$a, 2b$	a, b	Extrapolated
108	0·00	665·744	664·669	664·671	664·122	663·914
	0·15	566·143	566·175	566·175	566·183	566·186
	1·00	378·195	378·195	378·196	378·196	378·196
140	0·00	436·982	432·805	432·809	431·395	430·891
	0·15	373·270	373·833	373·829	373·966	374·011
	1·00	188·256	188·259	188·253	188·252	188·252
x	$\frac{R}{R_b}$	v				
		$\delta x = a, \delta\zeta = 4b$	$0{\cdot}5a, 2b$	$a, 2b$	a, b	Extrapolated
108	0·05	199·200	197·915	197·915	197·493	197·343
	0·15	239·986	239·966	239·966	239·960	239·958
	1·00	207·745	207·745	207·745	207·745	207·745
140	0·05	162·233	159·922	159·924	159·078	158·772
	0·15	196·914	196·704	196·703	196·647	196·628
	1·00	154·816	154·820	154·820	154·820	154·820
x		R_b				
		$\delta x = a, \delta\zeta = 4b$	$0{\cdot}5a, 2b$	$a, 2b$	a, b	Extrapolated
108		19·5463	19·5463	19·5463	19·5463	19·5463
124		22·2490	22·2490	22·2491	22·2491	22·2491
140		26·2288	26·2281	26·2282	26·2281	26·2281

TABLE 2

Effect of Mesh Size on Computed Values for a Vortex in a Pipe

$\delta x = f_1$; δx = 0·3125(4), 0·625(2), 1·25(2), 2·5(4), 5(4), 10(4).

$\delta x = f_2$; δx = 0·625(4), 1·25(2), 2·5(2), 5(1), 10(2), 20(2).

$\delta\zeta \propto b$, b = 0·0559017.

x	R	u					
		$\delta x = f_1$, $\delta\zeta = 4b$	$f_2, 2b$	$f_1, 2b$	f_1, b	Extrapolated	Hagen Poiseuille
5	0	29·167	28·912	28·914	28·768	28.712	
	0·44721	28·861	28·603	28·604	28·457	28·401	
	1·11803	25·284	25·002	25·005	24·861	24·806	
	1·78885	13·323	13·144	13·148	13·065	13·034	
75	0	34·232	33·686	33·683	33·438	33·347	33·333
	0·44721	32·863	32·339	32·335	32·100	32·013	32·000
	1·11803	25·674	25·265	25·262	25·078	25·010	25·000
	1·78885	12·324	12·129	12·126	12·037	12·004	12·000
x	R	v					
		$\delta x = f_1$, $\delta\zeta = 4b$	$f_2, 2b$	$f_1, 2b$	f_1, b	Extrapolated	
5	0·44721	2·153	2·091	2·091	2·071	2·064	
	1·11803	2·988	2·948	2·948	2·932	2·926	
	1·78885	1·303	1·299	1·300	1·298	1·297	
x		P_{wall}				$(\Delta P/\Delta x)_{\text{wall}}$	
	$\delta x = f_1$, $\delta\zeta = 4b$	$f_2, 2b$	$f_1, 2b$	f_1, b	Extrapolated	Extrapolated	Hagen Poiseuille
5	8110·81	8119·99	8119·90	8124·59	8126·37		
10	7949·04	7962·83	7962·76	7969·20	7971·61		
35	7247·74	7274·66	7274·89	7286·97	7291·47		
45	6973·74		7005·29	7019·24	7024·43	26·703	26·667
55	6699·88	6735·90	6735·85	6751·84	6757·79	26·664	26·667
65	6426·01		6466·36	6484·20	6490·84	26·695	26·667
75	6152·15	6196·78	6196·92	6216·80	6224·20	26·664	26·667

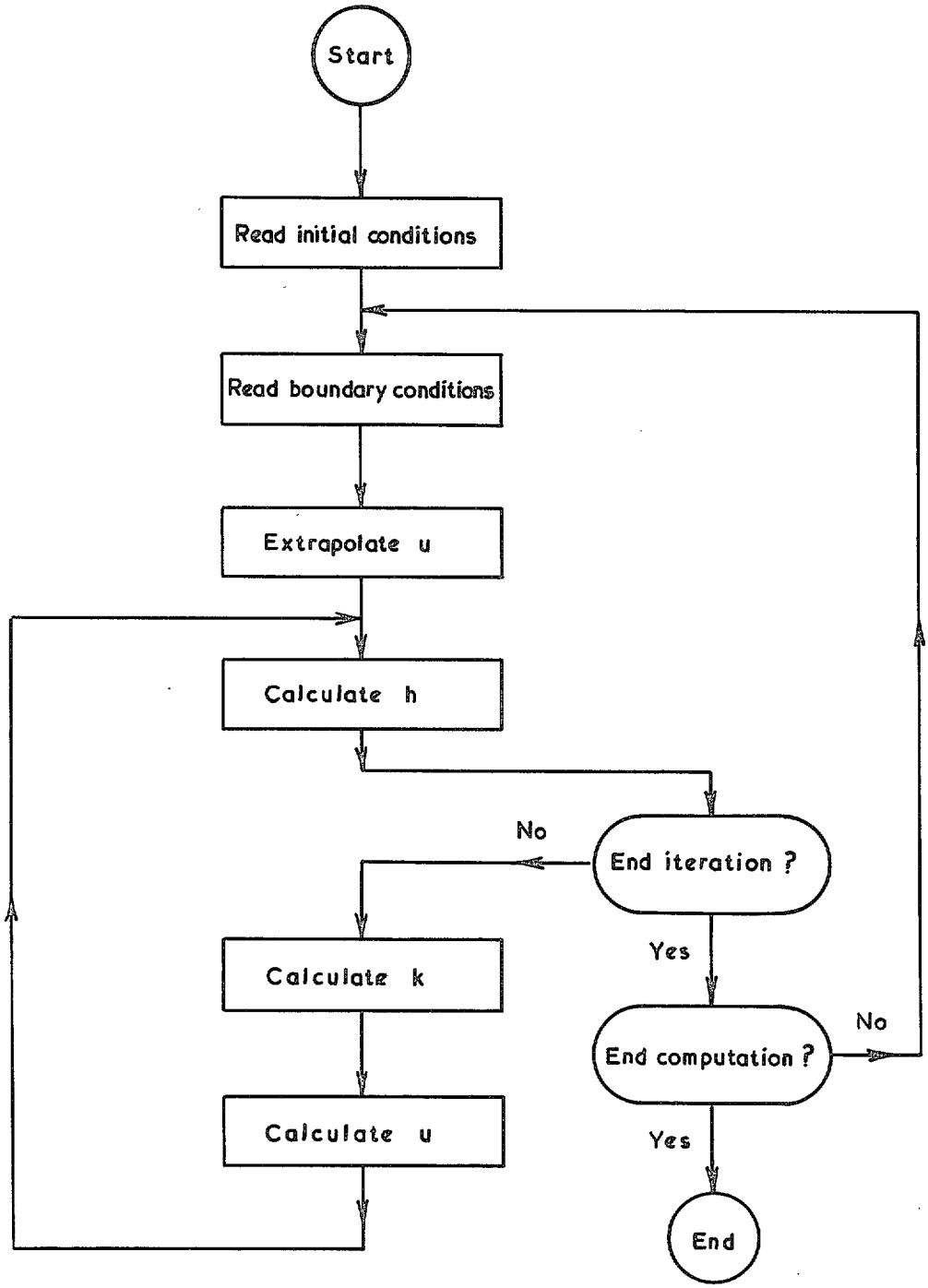

FIG. 1. Simplified diagram of computer programme.

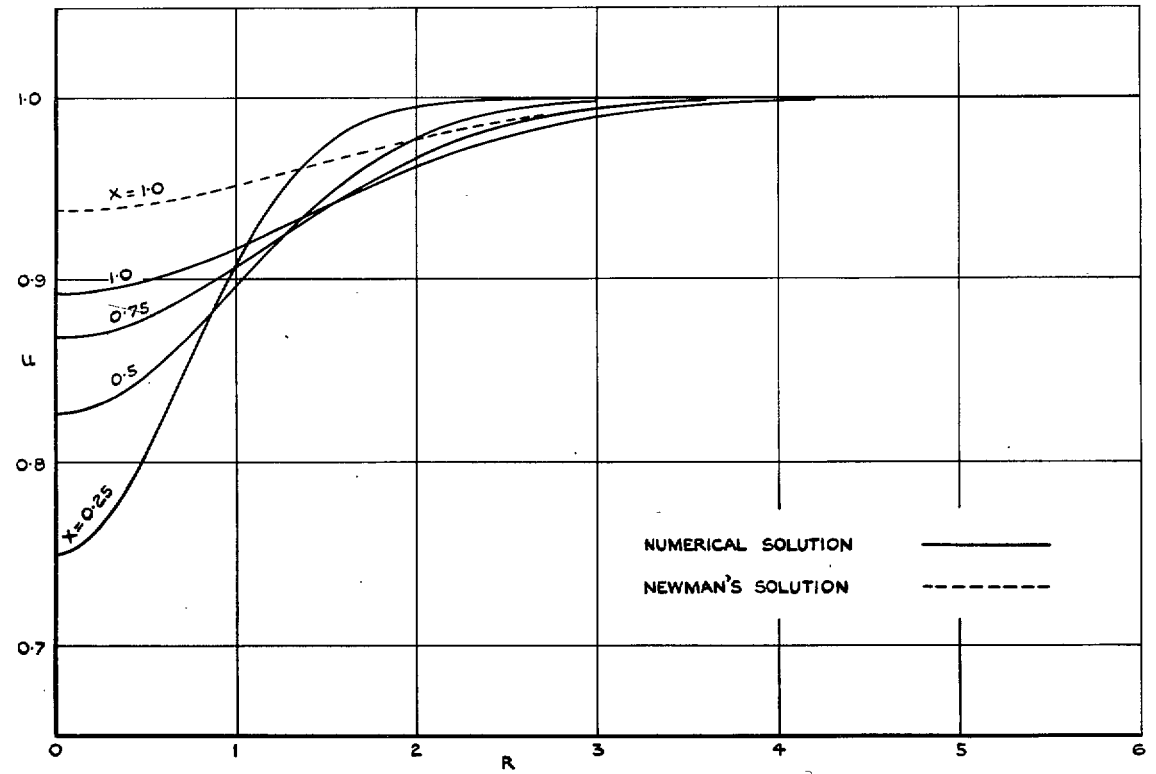

FIG. 2. Profiles of axial velocity in a trailing vortex.

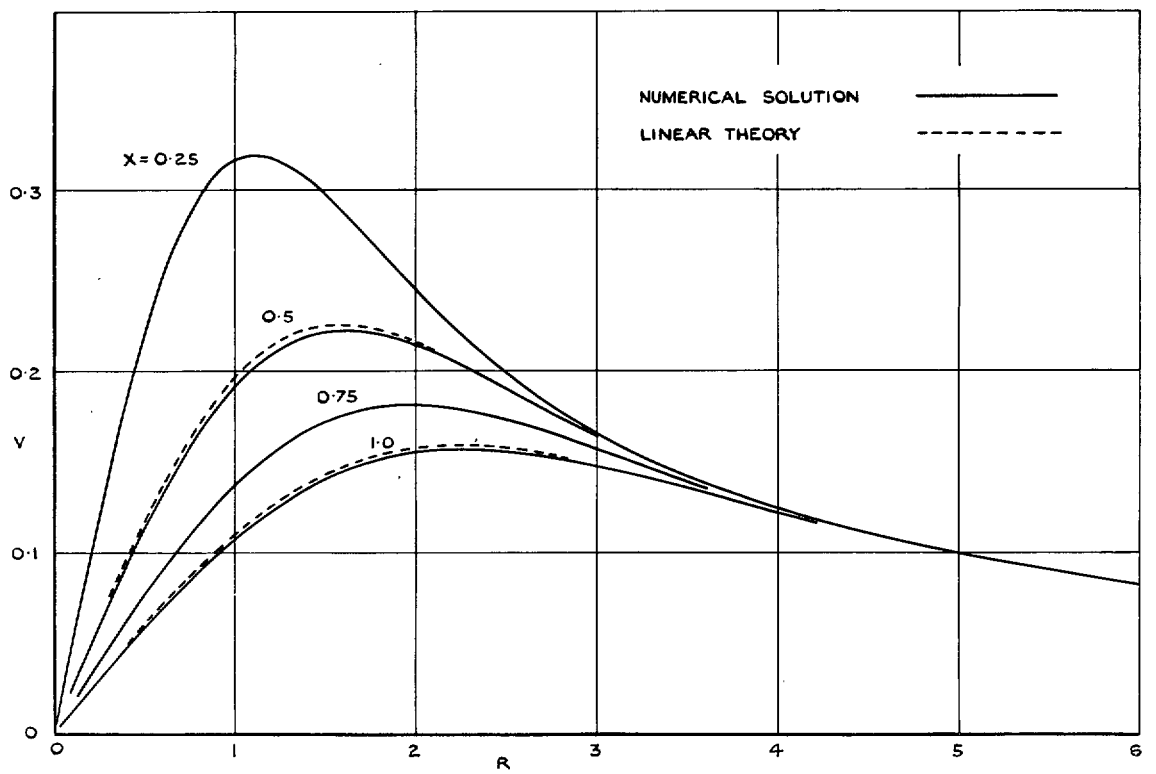

FIG. 3. Profiles of circumferential velocity in a trailing vortex.

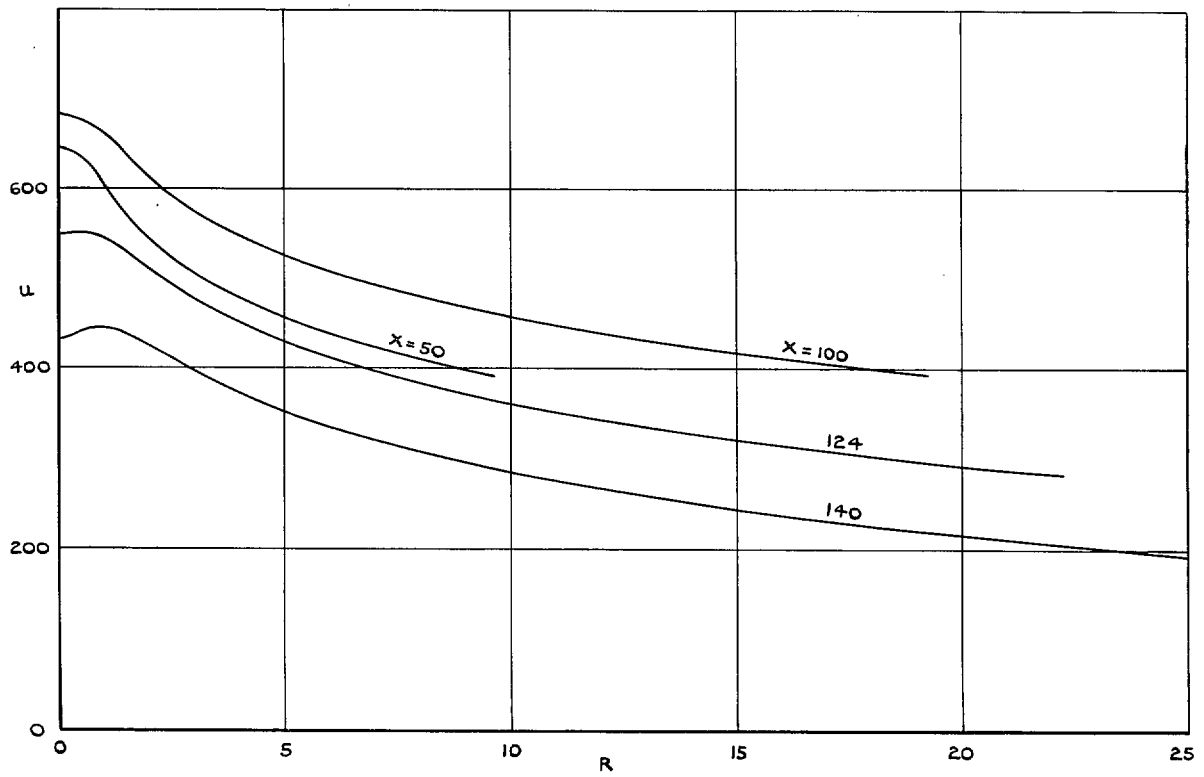

FIG. 4. Profiles of axial velocity in a leading-edge vortex.

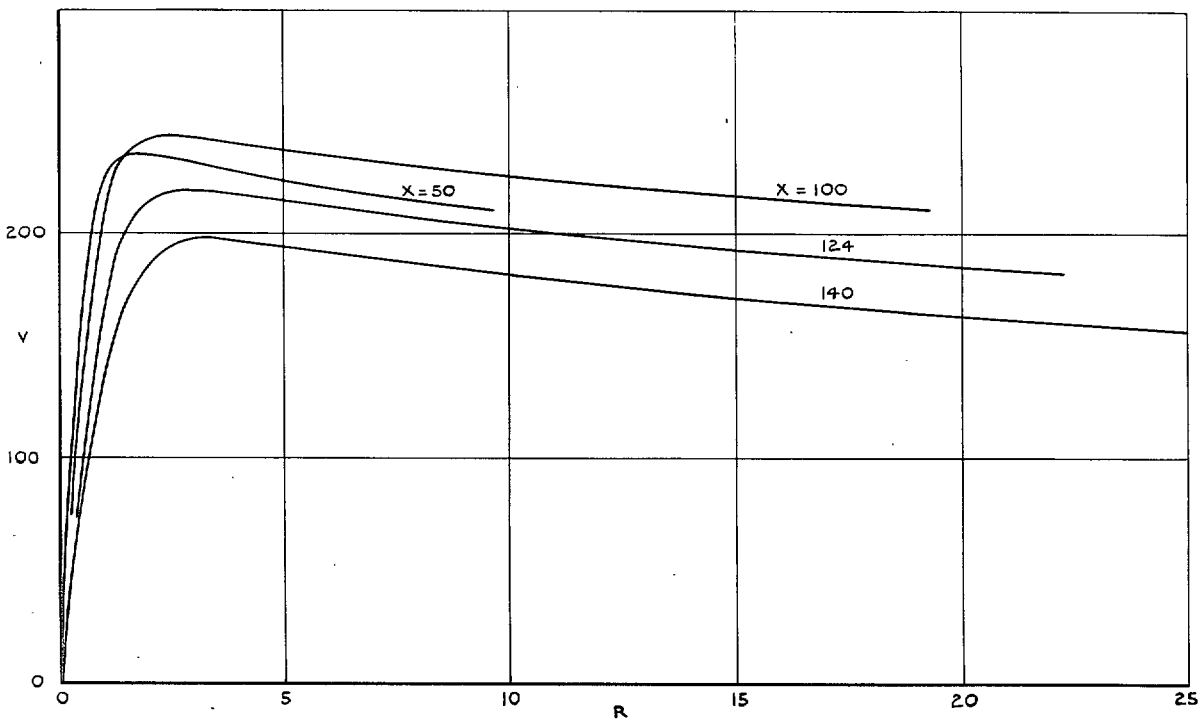

FIG. 5. Profiles of circumferential velocity in a leading-edge vortex.

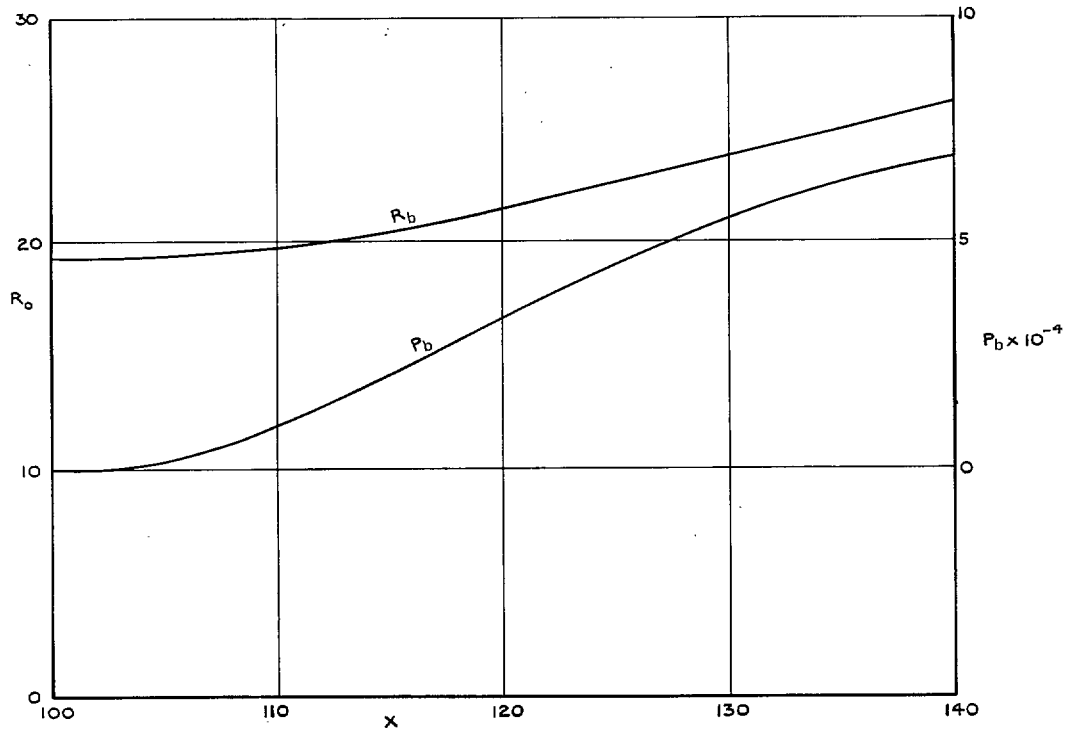

6. The computed radius R_b of the bounding stream-tube of a leading-edge vortex and the prescribed pressure P_b on the bounding stream-tube.

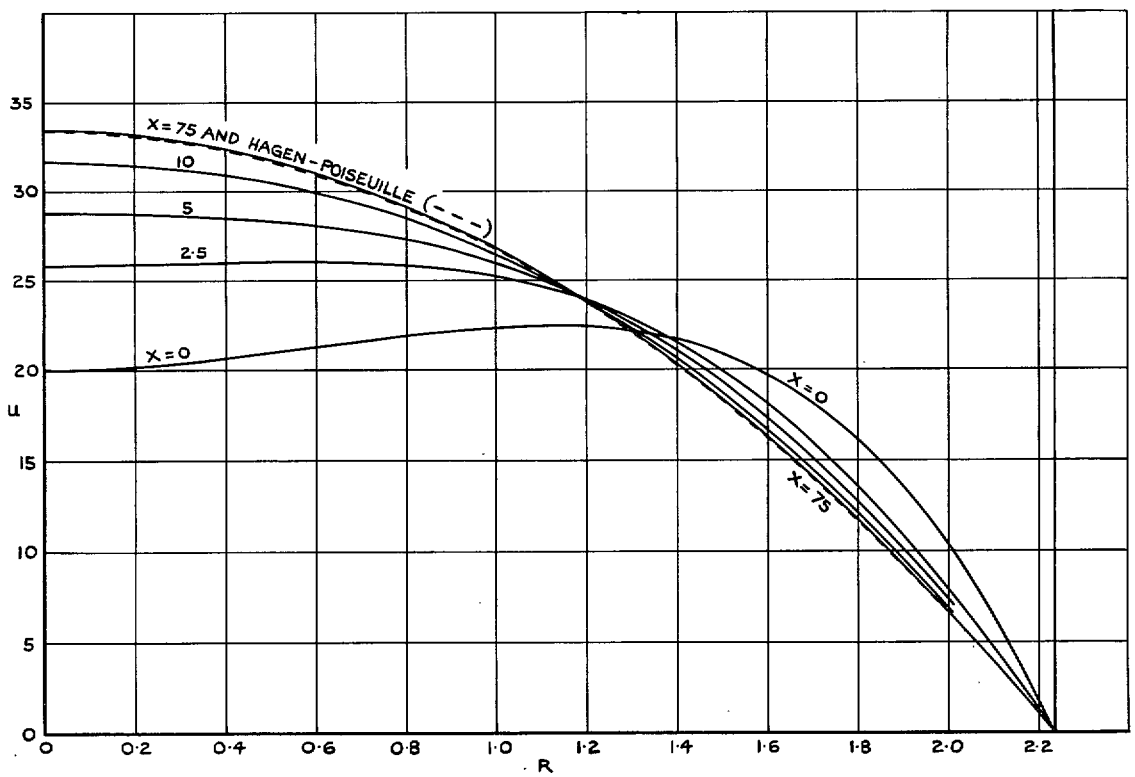

FIG. 7. Profiles of axial velocity for a vortex in a pipe.

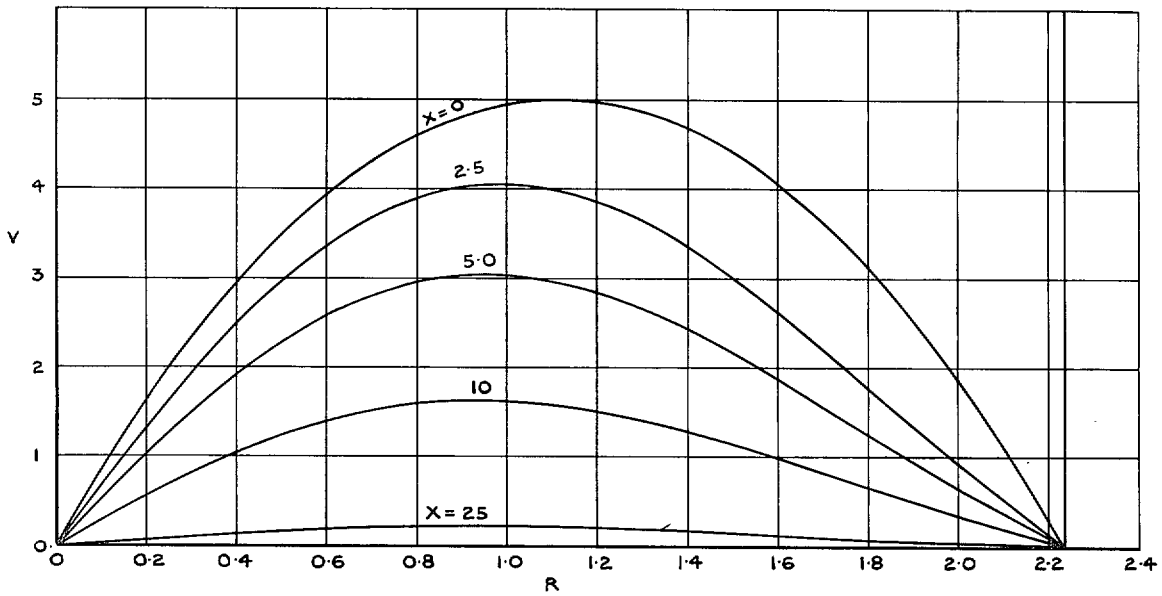

FIG. 8. Profiles of circumferential velocity for a vortex in a pipe.

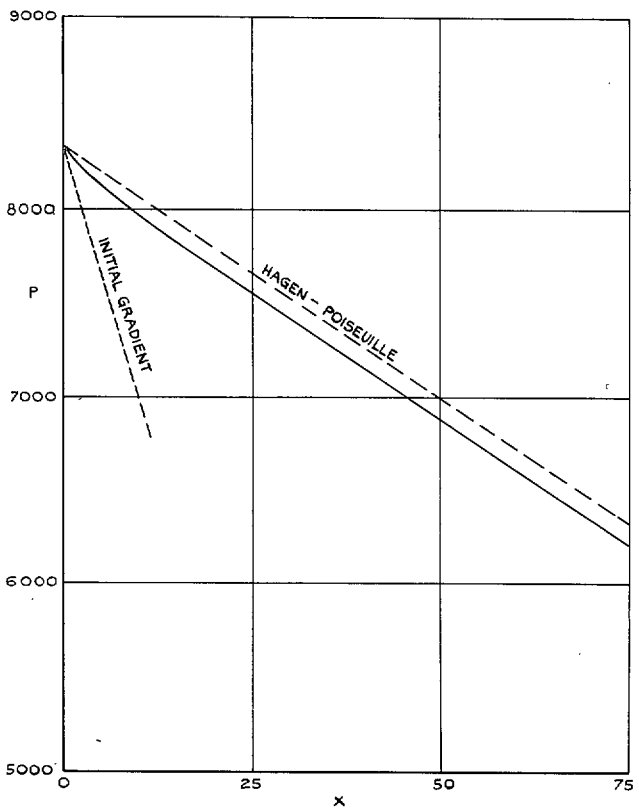

FIG. 9. Pressure distribution on the wall of a pipe.

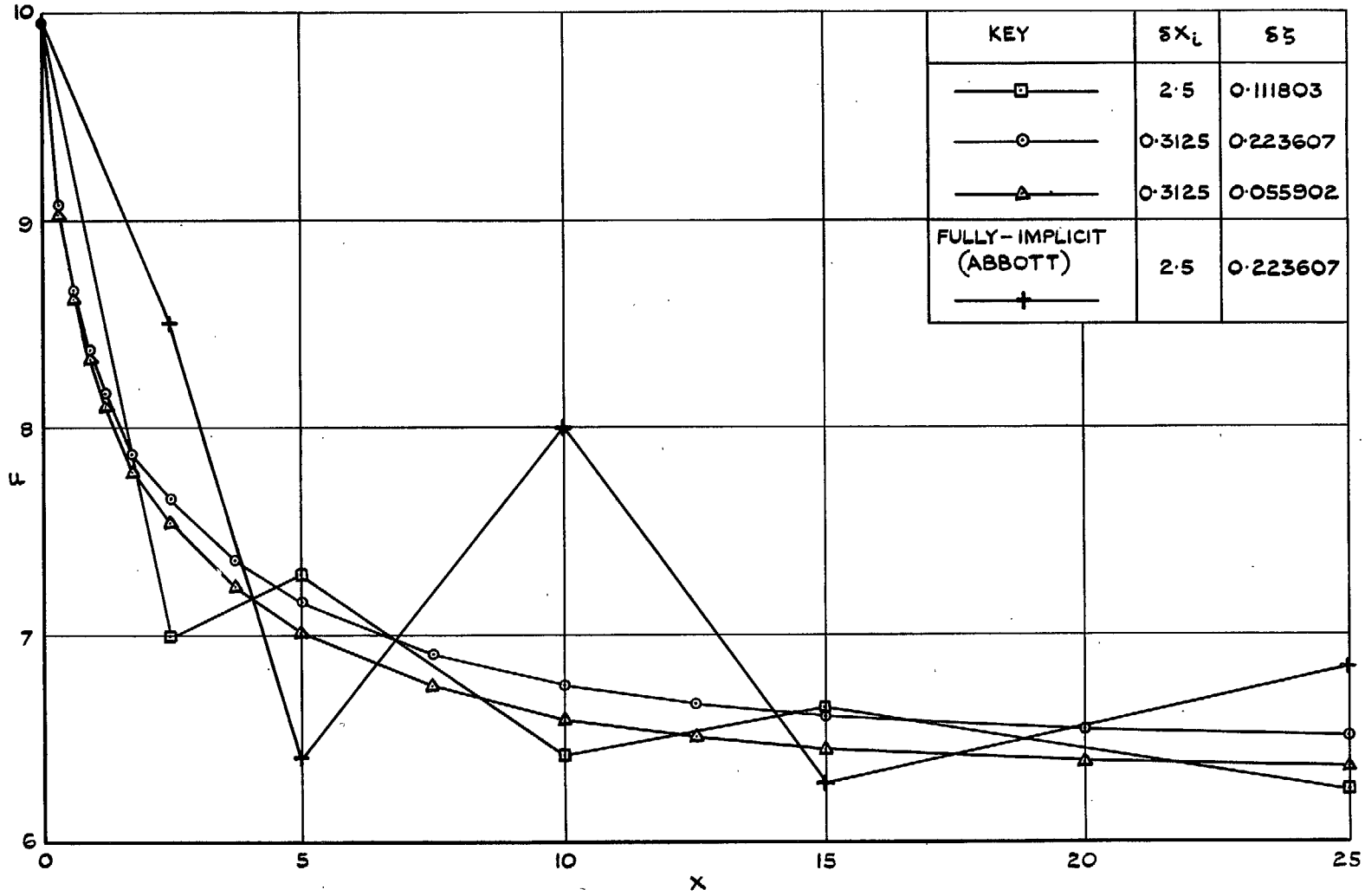

FIG. 10. Variations along a pipe of axial velocity u near the wall.

Printed in Wales for Her Majesty's Stationery Office by Allens Printers (Wales) Limited
Dd.129527. K5. 6/67

Published by
HER MAJESTY'S STATIONERY OFFICE

To be purchased from
49 High Holborn, London W.C.1
423 Oxford Street, London W.1
13A Castle Street, Edinburgh 2
109 St. Mary Street, Cardiff CF1 1JW
Brazennose Street, Manchester 2
50 Fairfax Street, Bristol 1
258/259 Broad Street, Birmingham 1
7–11 Linenhall Street, Belfast BT2 8AY
or through any bookseller

S.O. Code No. 23-3467